Solid-State Electronics 198 (2022) 108461

Contents lists available at ScienceDirect

Solid State Electronics

journal homepage: www.elsevier.com/locate/sse

Electron-phonon calculations using a Wannier-based supercell approach: Applications to the monolayer MoS_2 mobility☆

Jonathan Backman *, Youseung Lee, Mathieu Luisier

Integrated Systems Laboratory, ETH, Gloriastrasse 35, 8092 Zurich, Switzerland

ARTICLE INFO

Keywords:
Ab initio
Carrier transport
DFT
Electron-phonon interaction
Electron mobility
MoS_2

ABSTRACT

We present a first-principles method to calculate electron-phonon coupling elements in atomic systems, and showcase its application to the evaluation of the phonon-limited mobility of n-type single-layer MoS_2. The method combines a density functional theory (DFT) plane-wave supercell approach with a real-space maximally localized Wannier basis. It enables the calculation of electronic structure, phonon displacements with their corresponding frequencies, and real-space electron-phonon coupling elements on the same footing, without the need for density functional perturbation theory (DFPT) or Wannier interpolation. We report a low-field, intrinsic mobility of 274 cm^2/Vs at room temperature for MoS_2, and highlight its dependence on carrier density and temperature. In addition, we compare our findings to the latest available modeling data and put them in perspective with the experimentally measured values. Based on these observations, the mobilities presented in this work appear to be compatible with experimental results, when taking into account other scattering sources. Hence, the proposed approach provides a reliable framework for mobility calculations that can be extended towards large-scale device simulations.

1. Introduction

Recent advances in density functional theory (DFT) have enabled the theoretical study of electron-phonon (el-ph) interactions in various semiconductors. The developed approaches have been extended to the calculation of the carrier mobility of these materials, in particular two-dimensional (2-D) transition metal dichalcogenide (TMD) monolayers. Indeed 2-D TMD-based transistors are widely seen as one of the most promising candidates for future logic switches. Among them, field-effect transistors (FETs) made of MoS_2 monolayers have been shown to reach high ON-state currents [1]. To better understand the physics behind carrier transport in MoS_2 FETs, we showcase here an original Wannier-based supercell approach to calculate the MoS_2 mobility and its possible extension towards realistic device simulations. When deriving the method, we found that the inclusion of long-range interactions through an analytic expression of the 2-D Fröhlich [2] has a negligible effect on the total mobility value of MoS_2. We provide an overview of the el-ph-limited mobility in MoS_2 by comparing our results to available modeling data [3–11], thus showing that our results are in good agreement with the literature [11]. We also put our findings and the available data in perspective with the experimentally measured values.

2. Method

The el-ph coupling elements $g(k,q)$ can be expressed in terms of the electronic Hamiltonian derivatives with respect to atomic displacements, i.e. dH/dQ as [7]

$$g^{\lambda}_{nm}(\mathbf{k},\mathbf{q}) = \sum_{Iv} \frac{\partial H_{nm}}{\partial Q_{Iv}}(\mathbf{k}) f^{\lambda}_{Iv}(\mathbf{q}) \sqrt{\frac{\hbar}{2M_I\omega_{\lambda}(\mathbf{q})}} e^{i\mathbf{q}(\mathbf{R}_I-\mathbf{R}_0)}. \quad (1)$$

Here n/m are the orbital indices, λ (ω) the phonon mode index (energy), while $\mathbf{k}/\mathbf{q}$ are the el and ph Bloch vectors. Q_{Iv} represents the displacement of atom I along the direction v, M_I the displaced ion mass, $\mathbf{R}$ the unit cell lattice vector, f^{λ}_{Iv} the phonon displacement vector, and $\frac{\partial H_{nm}}{\partial Q_{Iv}}$ the dH/dQ elements. A DFT finite difference supercell approach can be employed to calculate dH/dQ on a real-space grid, after the DFT Hamiltonians, obtained with VASP [12] for a number of atomic displacements, have been transformed into a localized Wannier basis [13] such as

$$\frac{\partial H_{nm}}{\partial Q_{Iv}} = \frac{[H_{nm}(Q_{Iv}) - H_{nm}(-Q_{Iv})]}{2Q_{Iv}}. \quad (2)$$

By taking into account the symmetry of the system and equivalent atoms, the total number of required displacements can be significantly

☆ The review of this paper was arranged by Cristina Medina-Bailon.

* Corresponding author.
E-mail address: jbackman@iis.ee.ethz.ch (J. Backman).

https://doi.org/10.1016/j.sse.2022.108461

Available online 23 September 2022

reduced. This is done using the Phonopy code [14], which constructs a supercell, by repeating the unit cell along the directions of the primitive lattice vectors, for each unique displacement in the unit cell. By resorting to the same procedure, Force Constants are also obtained from the calculated forces of each displaced supercell using Phonopy.

A correction originating from the modified orbital overlaps must be included to account for the change in the basis functions associated with each displacement. Following Frederiksen et al. [15], an expression for the dH/dQ elements can be rewritten with correction terms as

$$\frac{\partial H_{nm}}{\partial Q_{Iv}} = \langle n|\frac{\partial \mathbf{H}}{\partial Q_{Iv}}|m\rangle = \frac{\partial\langle n|\mathbf{H}|m\rangle}{\partial Q_{Iv}} - \sum_{kl}\langle n'|k\rangle(\mathbf{S}^{-1})_{kl}\langle l|\mathbf{H}|m\rangle + \langle n|\mathbf{H}|k\rangle(\mathbf{S}^{-1})_{kl}\langle l|m'\rangle, \tag{3}$$

where the first term is the un-corrected dH/dQ elements, as obtained with finite difference, while the second term is the correction. Here, $\mathbf{S}$ is the orbital overlap matrix, $\langle n'|k\rangle$ and $\langle l|m'\rangle$ are derivatives of the orbital overlaps, and $\mathbf{H}$ represents the Hamiltonian of the un-displaced supercell. The overlap derivatives are calculated using finite differences based on the real-space Wannier functions. However, since the Wannier functions are constructed to be orthogonal, the overlap matrix is close to the identity matrix, resulting in a small contribution from this correction.

Once the corrected elements are calculated, symmetry operations are applied to build a complete set of dH/dQ elements corresponding to all possible displacements in the unit cell. Furthermore, numerical errors are minimized by averaging over symmetrically equivalent dH/dQ elements,

$$\frac{\partial H_{nm}}{\partial Q_{Iv}} = \frac{1}{N_S}\sum_{S}\frac{H^{S}_{nm}}{Q_{Iv}}, \tag{4}$$

where S indicates symmetrically equivalent dH/dQ elements and N_S is the number of symmetry operations.

The Wannier functions are by construction highly localized, meaning that the Hamiltonian elements quickly decay as the interacting orbitals are located further apart. This property transfers to the dH/dQ elements which are, in addition, localized around the displaced atom, as depicted in Fig. 1. The localized nature of the dH/dQ is essential in reducing the computational cost of transport calculations by truncating longer range interactions.

The Force Constants obtained from the displacement calculations, the unit cell Hamiltonian, and the dH/dQ can altogether be used to calculate $g(k,q)$. Subsequently, transport calculations based on the linearized Boltzmann Transport Equation (LBTE) or on the Non-equilibrium Green's Function (NEGF) formalism with dedicated scattering self-energies are possible, as illustrated in Fig. 2.

A key feature of this approach to calculate the real-space el-ph coupling elements is that no el-ph specific implementation is needed in the DFT code, contrary to density functional perturbation theory (DFPT) where el-ph Wannier interpolation is often needed to obtain matrix elements on a fine (k,q) grid. This method can therefore be used without modification for any plane-wave DFT code interfaced with Wannier90 or directly with a localized basis code.

3. Results

Each electronic structure calculation is performed with the generalized gradient approximation (GGA) of Perdew, Burke, and Ernzerhof (PBE) as implemented in VASP, using a k-point spacing smaller than 0.01 $Å^{-1}$, along each periodic direction, and a plane wave cutoff energy of 500 eV. Since the spin-orbit coupling has a negligible effect on the conduction band of MoS_2 it is omitted. The total energy convergence criterion is set to less than 10^{-10} eV. The unit cell is relaxed to ensure that the residual forces are bellow 10^{-8} eV/Å. Gaussian smearing is used with a smearing width of 0.05 eV. The Wannier Hamiltonian is obtained from the DFT calculations, by considering 5 d-like orbitals on each molybdenum atom and three p-like orbitals on each sulfur as starting guesses for the minimization procedure. Displacement calculations are performed with a $9 \times 9 \times 1$ supercell. A vacuum space of 20 Å is used in the z-direction, which is considered non-periodic. The displacement distance is 0.01 Å.

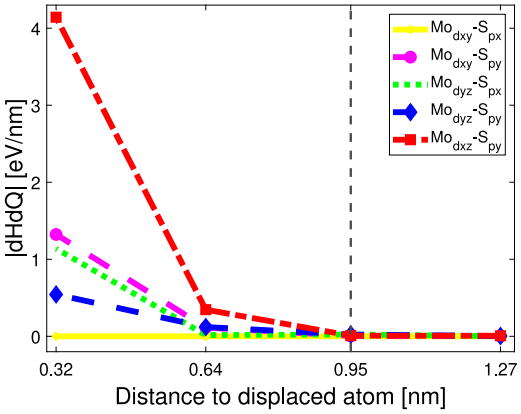

Fig. 1. Example of "dH/dQ vs distance of displaced atom" data, illustrating the localized nature of the elements.

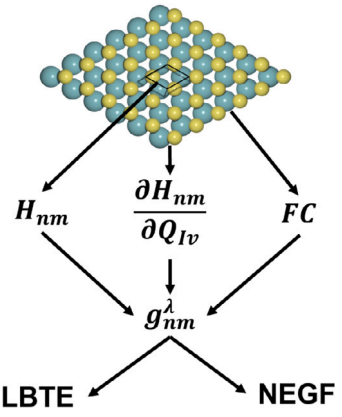

Fig. 2. Workflow showing the different steps of the method to compute the el-ph coupling elements used in the linearized Boltzmann Transport Equation (LBTE) and in the Non-equilibrium Green's Function (NEGF) formalism.

The electron and phonon bandstructure of monolayer MoS_2 are reported in Fig. 3. The convergence results for the $g(k,q)$ corresponding to the longitudinal optical phonon are also shown and compared to an analytical expression for the 2-D Fröhlich interaction. Convergence is tested by limiting the interaction range to that of smaller supercells. Absolute values of $g(k,q)$ calculated on a q-grid for a fixed k-point at the conduction band minimum are displayed in Fig. 4 for 4 different phonon modes. The subsequent mobility calculations are performed using an iterative LBTE solver [6,16] with the $g(k,q)$ calculated on a $201 \times 201 \times 1$ k/q-point grid in the full Brillouin Zone, including scattering states up to 0.4 eV above the conduction band minimum. The resulting mobility at different temperatures is plotted as a function of the carrier density in Fig. 5. The intrinsic mobility at room temperature is found to be 274 cm^2/Vs. We note that the mobility calculations with and without the 2-D Fröhlich contributions are almost identical (not shown here).

4. Benchmark

Table 1 summarizes the MoS_2 el-ph-limited mobility values extracted from several *ab initio* studies and compare them to those obtained in this work. In spite of numerous reports about the el-ph carrier

Table 1
Comparison between the MoS_2 mobility values collected from previous studies and those calculated in this work (marked in blue). The data is classified as a function of the electron density, from low intrinsic density to high (5e13 cm^{-2}). The extracted temperature-dependent exponents γ are provided, when available. The corresponding methods for the calculation of the electronic bandstructure and el-ph matrix elements are also given. Abbreviations: Frozen Phonon (FP), Linear Interpolation (LI), Wannier Interpolation (WI), Multi-Valley Deformation Potential (MVDP), Linear Combination of Atomic Orbitals (LCAO), Plane-Wave (PW), Local density approximation (LDA), Perdew-Burke-Ernzerhof (PBE), Spin-Orbit Coupling (SOC), Optimized Norm-Conserving Vanderbilt (ONCV), Quantum Espresso (QE).

Mobility [cm^2/Vs]				γ	DFT	El–Ph	Ref.
Intrinsic	n = 2e12	1e13	5e13 [cm^{-2}]		Bandstructure	Matrix Elements	
410	400	343	–	1.690	LCAO, LDA	FP	3
130	–	–	–		PW (QE), LDA	DFPT	4
225	–	–	–		PW (QE), PBE	DFPT	5
150	–	–	–		PW (QE), PBE	DFPT + LI	6
380	368	340	244	1.349	LCAO, PBE	FP (9×9)	7
–	–	–	144		PW (QE)	DFPT + LI	8
–	168	–	–	1.378	PW (QE), ONCV-PBE + SOC	DFPT + WI	9
147	–	–	–		PW (QE), ONCV-PBE	DFPT + WI	10
290	275	244	122		PW (QE)	MVDP	11
274	264	226	114	1.436	PW (VASP), PBE	FP (9×9)	This work

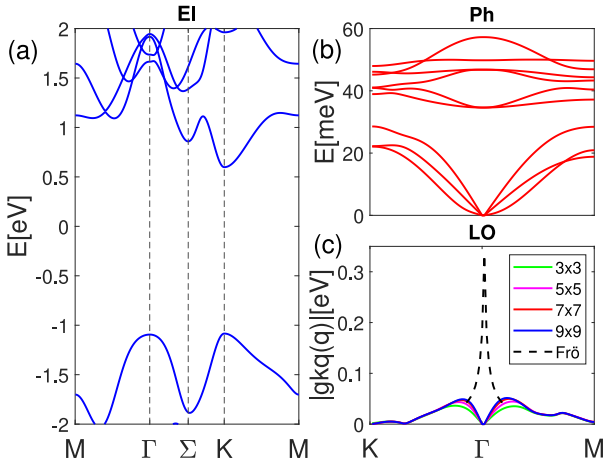

Fig. 3. (a) Electronic band structure, (b) phonon dispersion, (c) Fröhlich el-ph coupling elements along the k/q-points of high symmetry. The convergence of the long range interaction for different supercell size is compared to an analytical expression of the 2-D Fröhlich interaction (dashed line).

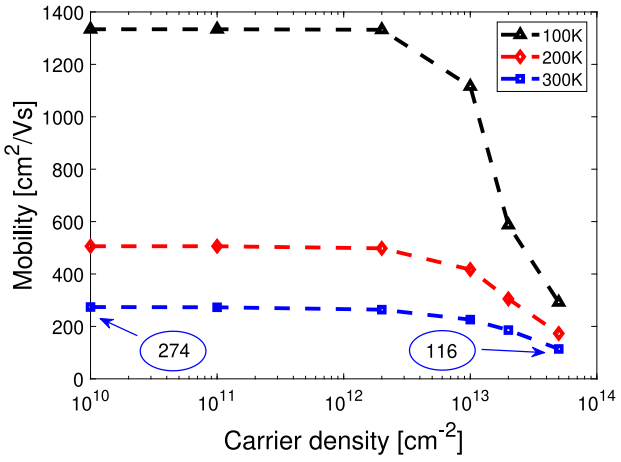

Fig. 5. 2-D MoS_2 phonon-limited mobility at different temperatures (100-300 K) as a function of the carrier density.

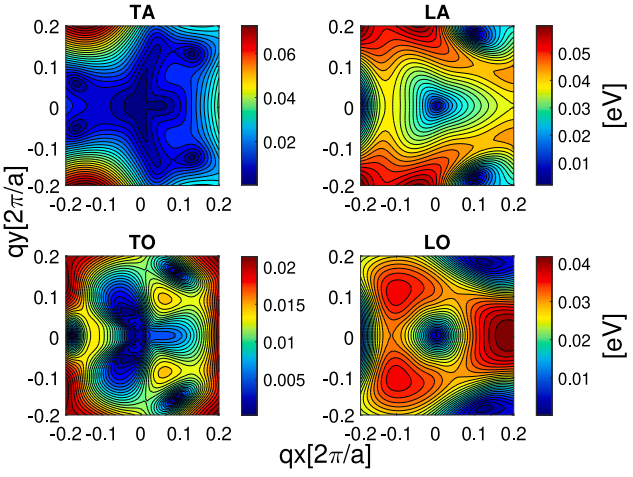

Fig. 4. El-ph coupling elements calculated on a q-grid for a fixed k-point at the conduction band minimum for 4 different phonon modes: transverse acoustic (TA), longitudinal acoustic (LA), transverse optical (TO), and longitudinal optical (LO).

mobility of MoS_2, no consensus exists about its "true" value. Mobilities ranging between 130 and 410 cm^2/Vs have been published. Recently, Ref. [10] suggested that the origin of those scattered values could be attributed to the choice of different pseudopotentials. From our review of the published data, we see no clear trend between the reported mobility values and model parameters such as pseudopotentials, exchange correlation, and perturbation method i.e. DFPT or frozen phonons (FP). We note however that other scattering mechanisms such as surface optical phonon and charged impurity scattering [16] are known to have a strong impact on the experimentally measured mobility of around 40 cm^2/Vs [17,18]. Moreover, it is expected that the MoS_2 intrinsic mobility without screening effects decreases at higher carrier concentrations due to enhanced intervalley scattering. Based on these observations, the mobility values presented in this work, including carrier and temperature dependencies, are compatible with experimental results and the expected decreases coming from the aforementioned scattering sources.

5. Outlook

With the calculated quantities constructed on a real space grid, the presented method can be directly used as input to a NEGF-based quantum transport device simulator. Using this, full devices can be simulated while considering dissipative transport, thus providing insight into effects such as self heating in 2D-FET devices.

Declaration of competing interest

The authors declare that they have no known competing financial interests or personal relationships that could have appeared to influence the work reported in this paper.

Acknowledgments

This research was funded by the Swiss National Science Foundation under grant No. 175479 (ABIME), and by the Swiss National Supercomputing Center under project s1119.

References

[1] O'Brien K, Dorow C, Penumatcha A, Maxey K, Lee S, Naylor C, Hsiao A, Holybee B, Rogan C, Adams D, et al. Advancing 2D monolayer CMOS through contact, channel and interface engineering. In: 2021 IEEE international electron devices meeting. IEEE; 2021, p. 1–7.

[2] Sohier T, Calandra M, Mauri F. Two-dimensional Fröhlich interaction in transition-metal dichalcogenide monolayers: Theoretical modeling and first-principles calculations. Phys Rev B 2016;94(8):085415.

[3] Kaasbjerg K, Thygesen KS, Jacobsen KW. Phonon-limited mobility in n-type single-layer MoS 2 from first principles. Phys Rev B 2012;85(11):115317.

[4] Li X, Mullen JT, Jin Z, Borysenko KM, Nardelli MB, Kim KW. Intrinsic electrical transport properties of monolayer silicene and MoS 2 from first principles. Phys Rev B 2013;87(11):115418.

[5] Restrepo OD, Krymowski KE, Goldberger J, Windl W. A first principles method to simulate electron mobilities in 2D materials. New J Phys 2014;16(10):105009.

[6] Li W. Electrical transport limited by electron-phonon coupling from Boltzmann transport equation: An ab initio study of Si, Al, and MoS 2. Phys Rev B 2015;92(7):075405.

[7] Gunst T, Markussen T, Stokbro K, Brandbyge M. First-principles method for electron-phonon coupling and electron mobility: Applications to two-dimensional materials. Phys Rev B 2016;93(3):035414.

[8] Sohier T, Campi D, Marzari N, Gibertini M. Mobility of two-dimensional materials from first principles in an accurate and automated framework. Phys Rev Mater 2018;2(11):114010.

[9] Zhou J-J, Park J, Lu I-T, Maliyov I, Tong X, Bernardi M. Perturbo: A software package for ab initio electron-phonon interactions, charge transport and ultrafast dynamics. Comput Phys Comm 2021;264:107970.

[10] Gaddemane G, Gopalan S, Van de Put ML, Fischetti MV. Limitations of ab initio methods to predict the electronic-transport properties of two-dimensional semiconductors: the computational example of 2H-phase transition metal dichalcogenides. J Comput Electron 2021;20(1):49–59.

[11] Pilotto A, Khakbaz P, Palestri P, Esseni D. Semi-classical transport in MoS2 and MoS2 transistors by a Monte Carlo approach. Solid-State Electron 2022;192:108295.

[12] Kresse G, Furthmüller J. Efficient iterative schemes for ab initio total-energy calculations using a plane-wave basis set. Phys Rev B 1996;54(16):11169.

[13] Marzari N, Vanderbilt D. Maximally localized generalized Wannier functions for composite energy bands. Phys Rev B 1997;56(20):12847.

[14] Togo A, Tanaka I. First principles phonon calculations in materials science. Scr Mater 2015;108:1–5.

[15] Frederiksen T, Paulsson M, Brandbyge M, Jauho A-P. Inelastic transport theory from first principles: Methodology and application to nanoscale devices. Phys Rev B 2007;75(20):205413.

[16] Lee Y, Fiore S, Luisier M. Ab initio mobility of single-layer MoS 2 and WS 2: comparison to experiments and impact on the device characteristics. In: 2019 IEEE international electron devices meeting. IEEE; 2019, p. 4–24.

[17] Radisavljevic B, Kis A. Mobility engineering and a metal–insulator transition in monolayer MoS2. Nature Mater 2013;12(9):815–20.

[18] Smithe KK, English CD, Suryavanshi SV, Pop E. High-field transport and velocity saturation in synthetic monolayer MoS2. Nano Lett 2018;18(7):4516–22.